



<http://www.diva-portal.org>

Postprint

This is the accepted version of a paper published in *Journal of Applied Physics*. This paper has been peer-reviewed but does not include the final publisher proof-corrections or journal pagination.

Citation for the original published paper (version of record):

Lykissa, I., Li, S., Ramzan, M., Chakraborty, S., Ahuja, R. et al. (2014)

Electronic density-of-states of amorphous vanadium pentoxide films: Electrochemical data and density functional theory calculations.

Journal of Applied Physics, 115(18): 183701/1-/5

<http://dx.doi.org/10.1063/1.4875636>

Access to the published version may require subscription.

N.B. When citing this work, cite the original published paper.

Permanent link to this version:

<http://urn.kb.se/resolve?urn=urn:nbn:se:uu:diva-228477>

Electronic density-of-states of amorphous vanadium pentoxide films: Electrochemical data and density functional theory calculations

Iliana Lykissa¹, Shu-Yi Li¹, Muhammad Ramzan², Sudip Chakraborty^{2,3},
Rajeev Ahuja^{2,3}, Claes G. Granqvist¹, and Gunnar A. Niklasson^{1,a)}

¹ *Department of Engineering Sciences, The Ångström Laboratory, Uppsala University, P.O. Box 534, SE-75121 Uppsala, Sweden*

² *Department of Physics and Astronomy, The Ångström Laboratory, Uppsala University, P.O. Box 516, SE-75120 Uppsala, Sweden*

³ *Applied Materials Physics, Department of Materials and Engineering, Royal Institute of Technology (KTH), SE-100 44 Stockholm, Sweden*

Thin films of V_2O_5 were prepared by sputter deposition onto transparent and electrically conducting substrates and were found to be X-ray amorphous. Their electrochemical density of states was determined by chronopotentiometry and displayed a pronounced low-energy peak followed by an almost featureless contribution at higher energies. These results were compared with density functional theory calculations for amorphous V_2O_5 . Significant similarities were found between measured data and computations; specifically, the experimental low-energy peak corresponds to a split-off part of the conduction band apparent in the computations. Furthermore, the calculations approximately reproduce the experimental band gap observed in optical measurements.

Author to whom correspondence should be addressed. Electronic mail: gunnar.niklasson@angstrom.uu.se

I. INTRODUCTION

Thin films of vanadium pentoxide, V_2O_5 , can be deposited by several methods and are of interest for a wide range of applications.¹ This material has a layered structure that serves well as a host for ion intercalation, and consequently V_2O_5 has been considered for uses in solid-state ionics, with cathodes in Li-ion batteries being one example.² Electrochromics, and its implementation in smart windows,^{3,4} is another area of interest for films of V_2O_5 (Refs. 5 and 6) and V_2O_5 - TiO_2 .^{7,8} Amorphous films showed weak modulation of their optical properties upon ion intercalation and have been studied as almost color-neutral counter electrodes in electrochromic devices.^{7,8} Nanostructured V_2O_5 films, on the other hand, can display strong electrochromism and yield high optical contrast between colored and bleached states.⁹ Recent results indicate that the thermochromic properties of vanadium pentoxide might be very sensitive to doping, and $V_2O_5:Mo$ is of possible interest for applications at ambient temperature.¹⁰ Still other potential uses for V_2O_5 films include gas sensors¹¹ and detectors for infrared radiation.¹²

A fundamental understanding of the electronic density-of-states (DOS) of V_2O_5 is important for several of the applications mentioned above. The reason for this importance is that intercalation of small positive ions, such as H^+ or Li^+ , leads to simultaneous insertion of charge-balancing electrons into unoccupied states with ensuing displacement of the Fermi level. These inserted electrons give rise to changes in the optical absorption in the film, *i.e.*, to electrochromism. Specifically, ion and electron insertion decreases the optical absorption of crystalline V_2O_5 in the ultraviolet and short-wavelength parts of the luminous spectrum, while the absorption increases at longer wavelengths of this spectrum and in the near-infrared.^{6,13} Amorphous V_2O_5 films, on the other hand, exhibit small changes of their optical properties.⁶

Electrochemical measurements can be used to elucidate the electronic properties of intercalation materials, and the energy distribution of the inserted ions can produce an image of the DOS in the low-energy part of the conduction band under the presumption that a rigid-band approximation is appropriate for the intercalation.^{14,15} This technique to infer DOSs was first tested with good results on amorphous thin films¹⁴ but appears to function also for nanocrystalline materials provided that no phase transition occurs during the intercalation.¹⁶ In an actual experiment, the intercalated ions may not have time enough to penetrate the entire film, and hence the measured electrochemical density-of-states (EDOS) is often of lower

magnitude than the one obtained from theoretical considerations. The electrochemical method is also able to give additional physical information on the pertinent ion insertion mechanism.¹⁶

This paper reports on the electronic density-of-states of sputter-deposited amorphous V₂O₅ thin films, as recorded by a chronopotentiometric technique employing Li⁺ ion intercalation. The measured EDOS was compared with theoretical results for amorphous V₂O₅, specifically obtained from *ab initio* molecular dynamics (MD) calculations. Qualitative agreement was observed among the two sets of data. The measured EDOS was also used to interpret the optical properties of as-deposited and ion-intercalated V₂O₅ films.

II. EXPERIMENTS

Vanadium pentoxide thin films were deposited by reactive DC magnetron sputtering from a 5-cm-diameter metallic vanadium target in a versatile deposition system based on a Balzers UTT 400 unit. The deposition took place in a gas mixture of oxygen and argon with an O₂ flow rate of 9.65 ml/min and an Ar flow rate of 80 ml/min. The pressure was approximately 16 mTorr during sputtering and the discharge power was 298 W. Films were deposited onto unheated glass substrates pre-coated with indium-tin-oxide (ITO) layers having a resistance of 60 Ω per square. Film thicknesses lay in the 110–200 nm range, as determined by surface profilometry using a Bruker DektakXT instrument.

X-ray diffractometry was performed on a Siemens D5000 instrument operating with CuK_α radiation at a wavelength of 1.54 Å. The detector had a parallel-plate collimator with an acceptance angle of 0.4°. Angles were scanned with intervals of 0.1° and a step-time of 2 s. Nothing but diffraction peaks due to ITO could be registered, and hence the V₂O₅ films were designated as X-ray amorphous.

Electrochemical measurements, specifically cyclic voltammetry (CV) and chronopotentiometry, were carried out in an Ar-filled glove box containing less than 2 ppm of water. V₂O₅ films were used as working electrodes in a three-electrode arrangement with metallic lithium foil serving as counter and reference electrodes. All electrodes were immersed in an electrolyte of 1 M LiClO₄ in propylene carbonate, which is suitable for Li⁺ intercalation into thin films. The electrochemical cell was controlled by an ECO Chemie Autolab/GPES interface. In the CV experiment, the voltage was swept linearly back and forth in the 2–4 V potential range while the current was measured. The sweep rate was 10 mV/s and measurements were conducted for ten cycles. Chronopotentiometry was performed by

applying a constant current I of $\sim 1 \mu\text{A}/\text{cm}^2$ between the working and counter electrodes and recording the potential U between these electrodes as a function of time t . This procedure resulted in electron and ion insertion into the V_2O_5 film comprising the working electrode. Chronopotentiometry data were taken for a wide range of intercalated ion concentrations; these measurements lasted for as much as ~ 28 h.

We define an intercalation parameter x as the number of Li^+ ions inserted per formula unit (f.u.) of V_2O_5 . It was calculated from the charge according to

$$x = \frac{ItM}{e\rho N_A Ad}, \quad (1)$$

where M is molar mass, ρ is the density of vanadium pentoxide, e is electron charge, N_A is Avogadro's number, A is electrode area and d is film thickness. The density of bulk V_2O_5 was used in the calculations. From the chronopotentiometry data we then obtained the derivative $-dx/dU$, where U is in units of eV; this derivative reflects the number of electrons (and ions) inserted into the film per energy unit and is identified as the EDOS.

Optical transmittance T and reflectance R were measured by spectrophotometry in the 350–2500-nm wavelength range for as-deposited and ion-intercalated samples. We used a Perkin–Elmer Lambda 900 instrument equipped with integrating sphere attachment and employed a Spectralon reflectance standard. The absorption coefficient α was obtained by the relation¹⁷

$$\alpha = \frac{1}{d} \ln \left(\frac{1-R}{T} \right). \quad (2)$$

III. CALCULATIONS OF ELECTRONIC STRUCTURE

A detailed understanding of the electrochemical properties of V_2O_5 requires knowledge of its electronic band structure, which in its turn depends on atomic arrangements. Bulk V_2O_5 forms a layer-type orthorhombic lattice with lattice constants $a = 11.512 \text{ \AA}$, $b = 3.564 \text{ \AA}$ and $c = 4.368 \text{ \AA}$,¹⁸ and the primitive cell contains two formula units (14 atoms). This cell consists of distorted corner-sharing and edge-sharing octahedra with each vanadium atom surrounded by six oxygen atoms. The octahedra are irregular with vanadium–oxygen separations varying from 1.58 to 2.79 \AA .¹⁸ The valence band consists primarily of O $2p$ states and the conduction band is dominated by V $3d$ states.

Calculations of the electronic structure of *crystalline* V_2O_5 have been performed recently

by Eyert and Höck¹⁹ who used density functional theory and local density approximation. We carried out analogous calculations using the generalized gradient approximation (GGA),²⁰ as implemented in the Vienna *Ab initio* Simulation Package (VASP) code,^{21,22} and obtained a DOS that was very similar to the one derived in earlier work.¹⁹ Structural optimization was done by use of $8 \times 8 \times 8$ *k*-points and energy cut-off at 600 eV. A mesh with $20 \times 20 \times 20$ *k*-points was used for DOS calculations.

In order to compare the present experiments with computations, it is necessary to model *amorphous* V₂O₅. Its density-of-states is expected to be different from that of the corresponding crystalline material, as can be inferred from ellipsometric data recorded in the luminous and ultraviolet spectral ranges for V₂O₅ films with varying degrees of crystallinity.²³ Our modeling of amorphous V₂O₅ departed from the corresponding crystalline material and used *ab initio* MD simulations, again as included in the VASP code.^{21,22} To avoid any memory of crystallinity, the fully melted system was first studied at 2000 K with 20-ps-long time steps, then 3000 more MD runs were performed with 3-ps-long steps to represent the system's evolution from 2000 to 300 K, and the last snapshot of this simulation was optimized at zero Kelvin in order to account for the fully quenched amorphous state. Finally we used the HSE06 method²⁴ with a $2 \times 1 \times 1$ super-cell to calculate DOS and band gap for amorphous V₂O₅. It should be noted that long-range order of atomic coordination is not present in the amorphous structure and the atoms form a continuous random network.

IV. RESULTS AND DISCUSSION

4.1 Electrochemical characterization

Figure 1 shows CV recordings pertaining to amorphous V₂O₅ films, specifically for the first and tenth voltammetric cycles. These data are in overall agreement with results from previous studies.⁶ Significant differences are found between the first and tenth cycle, but these differences are smaller than in prior work.⁶ In the present experiments, the CVs evolved during the first two cycles and then remained stable up to the tenth cycle. More charge was inserted into the film than was extracted from it during these initial cycles, which indicates irreversible Li⁺ intercalation during the CV measurements by up to $x = 0.16$ per f.u. of V₂O₅.

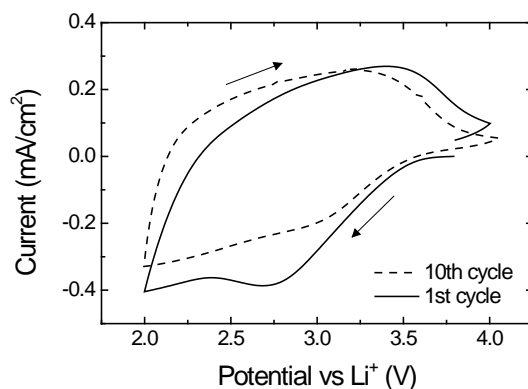


Fig. 1. Cyclic voltammograms showing current as a function of potential vs. Li⁺ for an amorphous V₂O₅ film. Data were taken at the first and tenth measurement cycle. Arrows indicate voltage sweep direction.

Figure 2 reports chronopotentiometry data on the potential for V₂O₅ films as a function of intercalation parameter x , which is directly proportional to time (*cf.* Eq. 1). The potential was significantly higher for as-deposited films than for films subjected to ten CV cycles. Specifically, the open-circuit voltage was 3.7 to 3.8 V for as-deposited and 3.3 to 3.4 V for cycled films. This difference indicates that the Fermi level lies at a higher energy in the cycled samples, which can be reconciled with the presence of irreversibly inserted Li⁺ ions and their associated charge-compensating electrons. The potential drops as x is increased because an increasing number of electrons are incorporated into the film, together with Li⁺ ions, and populate previously empty states in the conduction band of V₂O₅.

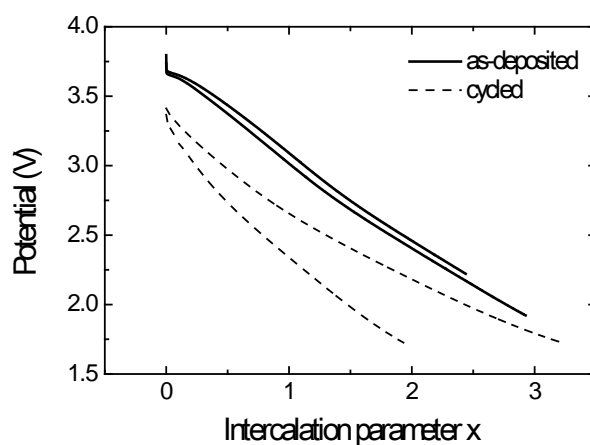


Fig. 2. Chronopotentiometry data on potential vs. Li⁺ as a function of intercalation parameter x for two as-deposited V₂O₅ films (solid curves) and for such films after ten voltammetric cycles (dashed curves).

4.2 Electron density-of-states: Experiments and calculation

Fig. 3 shows the computed total DOS in the valence and conduction bands of amorphous V_2O_5 , as well as the partial DOS due to O $2p$ and V $3d$ states. The band gap, i.e. the energy between the top of the valence band and the bottom of the conduction band was found to be ~ 2.4 eV. The valence band consists mainly of O $2p$ states, but the contribution from V $3d$ states is very significant. The conduction band has a dominant V $3d$ character with some admixture of O $2p$ states. The lower part of the conduction band exhibits a sharp peak, which is split off from the main part of the conduction band by a narrow gap of ~ 0.2 eV.

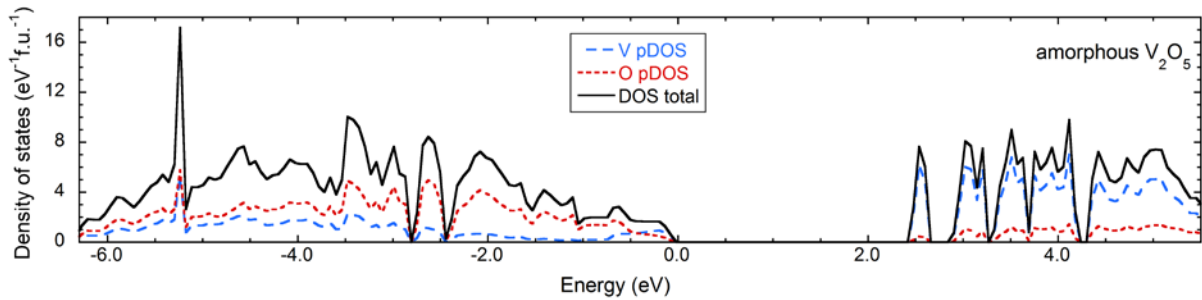


Fig. 3. Calculated electronic density of states, per formula unit, of amorphous V_2O_5 as a function of energy. The zero of energy was put at the top of the valence band. The curves denote the total DOS as well as the partial DOS from V and O atoms, as given in the figure.

The broad features seen in Fig. 2 can be amplified by differentiation and then give rise to a clear structure in the EDOS, as shown in Fig. 4(a) for two as-deposited V_2O_5 films. These data are compared with the total DOS, reported in Fig. 4(b), which shows an amplified view of part of the conduction band. The figures have been drawn so that the potential scale in Fig. 4(a) corresponds exactly to the energy scale in Fig. 4(b). Good correlation between the two sets of data is apparent for the lower part of the conduction band, where a narrow peak is prominent. Analysis of projected DOS yielded that this peak originates mainly from split-off V $3d$ states. The computed peak is separated from the main conduction band by a small band gap. Care must be exercised when interpreting the broad structure of the EDOS at energies higher than those of the first peak, and it should be noted that we have not used any phenomenological broadening function to smear the computed DOS data. However, large broadening effects are very likely to occur in disordered materials; in principle, they are energy dependent.²⁵

The EDOS in Fig. 4(a) contains about 0.16 electrons per f.u. in the sharp peak at low energies, and x is ~ 0.4 at an energy of ~ 0.3 eV from the band edge. Calculations, on the other hand, predict a split-off band with a width of ~ 0.25 eV containing one electron per f.u. Considering the entire energy range of ~ 1.8 eV, the EDOS measurements give $x \approx 2.8$, which can be compared with the theoretically expected value of $x \approx 8$. These discrepancies are probably associated with the slow kinetics of ion intercalation, and, within the experimental time frame, the Li^+ ions seem to permeate only part of the V_2O_5 film.

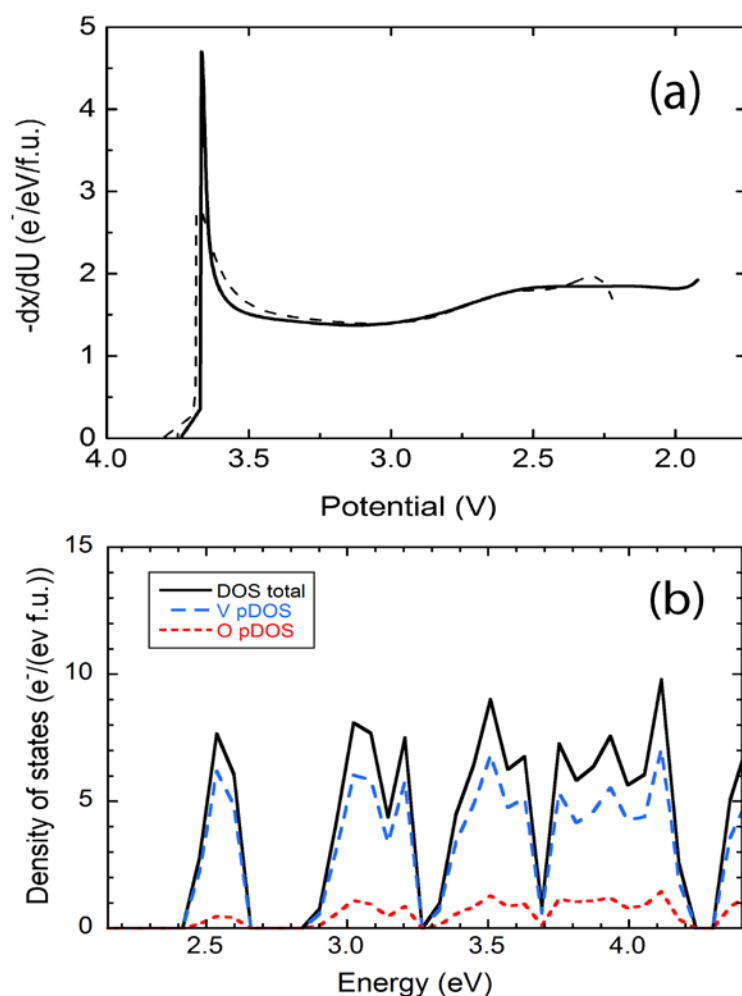


Fig. 4. Electrochemical density-of-states (EDOS) as a function of potential for two amorphous V_2O_5 films (a) and computed total density-of-states (DOS) for the same material (b). The energy (E) scale is the same as in Fig 3 and is related to the potential (U) scale by $E = 6.15 - U$. Note that the vertical scales are different for the two panels.

The sharp peak in the EDOS is present only for the first ion intercalation cycles. This is apparent from Fig. 5, which reports data for a V_2O_5 film in as-deposited state and for a similar film that has undergone ten CV cycles. The change in the EDOS can be associated with irreversibly incorporated Li^+ ions accompanied by the insertion of electrons filling the available electronic states in the peak so that subsequent electron insertion must start from a potential below this peak.

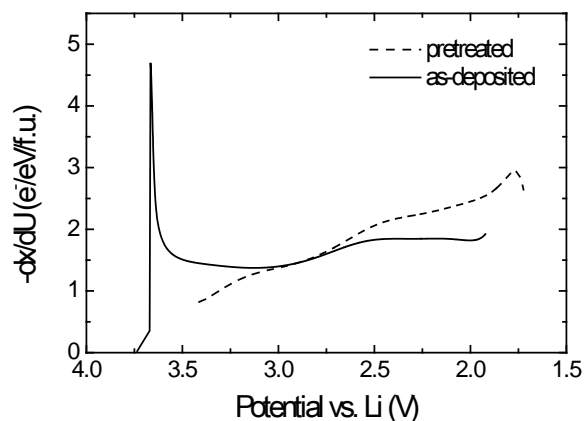


Fig. 5. Electrochemical density of states (EDOS) for an as-deposited V_2O_5 film and a similar, pretreated film that has undergone ten voltammetric cycles.

4.3 Optical absorption

Spectral optical recordings can give information that is complementary to electrochemical data, and Fig. 6 shows absorption coefficient for as-deposited and heavily ion-intercalated V_2O_5 films. The band gap E_g was found to be ~ 2.2 eV for the as-deposited film, which is consistent with earlier results.⁶ The spectral optical absorption of the intercalated films is broadened around the absorption edge, and it is not straightforward to obtain an accurate value of the band gap. It seems that E_g is only slightly increased upon intercalation, but it is important to observe that α is significantly diminished at energies above 2.4 eV in the intercalated films. An interpretation of these results in terms of electronic structure is hampered by the featureless character of the EDOS (*cf.* Fig. 4a). The decrease of α above 2.4 eV, and the minor change in E_g , probably are connected with the fact that intercalation of charge carriers occurs in only part of the film. When the latter situation is at hand, one would observe the same characteristics at and above the band gap, albeit with different strengths.

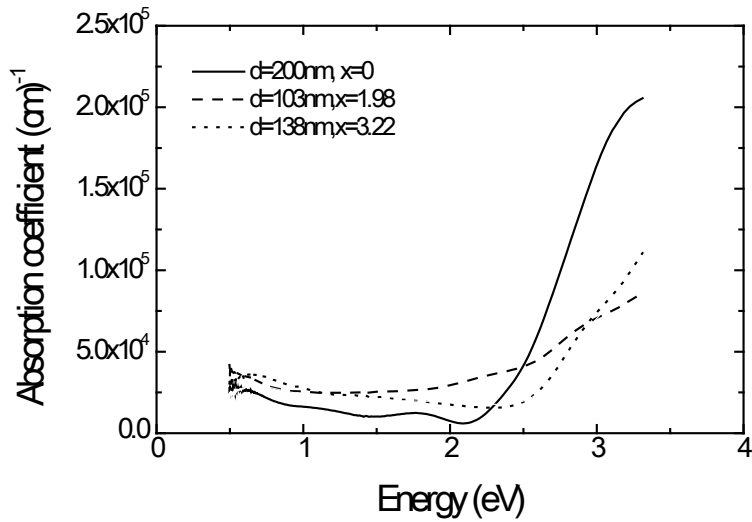


Fig. 6. Energy-dependent optical absorption coefficient for amorphous V_2O_5 thin films with different amounts of intercalated Li^+ ions. Film thickness and intercalation parameter are denoted d and x , respectively.

Figure 6 also shows significant absorption at energies below the band gap and that this absorption increases slightly towards lower energies. Absorption of this kind has been observed in previous work both for amorphous and crystalline V_2O_5 .⁶ It may be due to electronic transitions from localized states in the band gap to the conduction band or, at least for crystalline films, to small-polaron absorption.^{6,26} Vanadium pentoxide is known to be a material with strong electron-phonon interaction, and the existence of polarons as charge carriers have been inferred from electrical measurements and electron spin resonance.²⁷ We surmise that a polaron mechanism dominates also in amorphous V_2O_5 .

The low-energy absorption is significantly enhanced, but yet of the same order of magnitude, for ion-intercalated films. A growth of the absorption is expected since the Fermi energy in the intercalated films has increased and is situated in the conduction band thereby permitting an increased number of electronic transitions. However, the enhancement of the absorption is surprisingly small, which may indicate that the electronic states are localized in a large part of the conduction band for amorphous as well as ion-intercalated V_2O_5 films.

V. CONCLUSIONS

The electrochemically measured density-of-states in the conduction band of amorphous vanadium pentoxide shows a distinct peak close to the band edge, followed by a very broad

feature at higher energies. The first peak is consistent with computations for amorphous V_2O_5 which show a split-off part of the conduction band as a sharp maximum separated from the main part of the band by a small energy gap. At higher energies in the conduction band, however, the experiments do not display the peak structure apparent in the computations. These differences between experiment and theory are probably due to life-time broadening and may, at least in part, be a consequence of the small super-cell used in the computations for the amorphous structure (a larger super-cell would need an excessive computational time). The band gap of amorphous V_2O_5 was measured by to be ~ 2.2 eV, which is not far from the value ~ 2.4 eV found from the DOS of the amorphous structure.

In conclusion, the significant similarities between experimental EDOS and computed DOS that we observe indicate that the general methodology put forward in earlier work^{14,15} is a promising way to gain fundamental understanding of the properties of amorphous oxide thin films. Hence the present theory-coupled experimental investigation of V_2O_5 films is important for shedding light on the basic properties amorphous oxide thin films.

Acknowledgments

This work was partially supported by grants from the Swedish Research Council (VR) and the European Research Council under the European Community's Seventh Framework Program (FP7/2007–2013)/ERC Grant Agreement No. 267234 (GRINDOOR). IL's work at Uppsala University was supported by an Erasmus Student Mobility for Placement Grant, MR was supported by the Higher Education Commission (HEC) of Pakistan and SC was supported by Carl Trygger's Stiftelse för Vetenskaplig Forskning. We are grateful to SNIC and UPPMAX for allocating computing time for this project.

References

- ¹S. Beke, *Thin Solid Films* **519**, 1761 (2011).
- ²C. Navone, R. Baddour-Hadjean, J. P. Pereira-Ramos, and R. Salot, *J. Power Sources* **152**, A1790 (2005).
- ³C. G. Granqvist, *Handbook of Inorganic Electrochromic Materials* (Elsevier, Amsterdam, The Netherlands, 1995).
- ⁴C. G. Granqvist, *Solar Energy Mater. Solar Cells* **99**, 1 (2012); *Thin Solid Films* (2014), DOI:10.1016/j.tsf.2014.02.002.
- ⁵A. M. Andersson, C. G. Granqvist, and J. R. Stevens, *Appl. Opt.* **28**, 3295 (1989).
- ⁶A. Talledo and C. G. Granqvist, *J. Appl. Phys.* **77**, 4655 (1995).
- ⁷M. S. Burdis, *Thin Solid Films* **311**, 286 (1997); M. S. Burdis, J. R. Siddle, R.A. Batchelor, and J. M. Gallego, *Sol. Energy Mater. Sol. Cells* **54**, 93 (1998).
- ⁸S. Kim and M. Taya, *Solar Energy Mater. Solar Cells* **107**, 225 (2012).
- ⁹R. Maik, J. Scherer, L. Li, P. M. S. Cunha, O. A. Scherman, and U. Steiner, *Adv. Mater.* **24**, 1217 (2012).
- ¹⁰M. Nazemiyan and Y. S. Jalili, *AIP Adv.* **3**, 112103 (2013).
- ¹¹J. Liu, X. Wang, Q. Peng, and Y. Li, *Adv. Mater.* **17**, 764 (2005).
- ¹²H. K. Kang, Y. H. Han, H. J. Shin, S. Moon, and T. H. Kim, *J. Vac. Sci. Technol. B* **21**, 1027 (2003).
- ¹³M. Green and K. Pita, *J. Appl. Phys.* **81**, 3592 (1997).
- ¹⁴M. Strømme, R. Ahuja, and G. A. Niklasson, *Phys. Rev. Lett.* **93**, 206403 (2004).
- ¹⁵G. A. Niklasson, R. Ahuja, and M. Strømme, *Mod. Phys. Lett. B* **20**, 863 (2006).
- ¹⁶J. Backholm, P. Georén, and G. A. Niklasson, *J. Appl. Phys.* **103**, 023702 (2008).
- ¹⁷W.Q. Hong, *J. Phys. D: Appl. Phys.* **22**, 1384 (1989).
- ¹⁸R. Enjalbert and J. Galy, *Acta Cryst. C* **42**, 1467 (1986).
- ¹⁹V. Eyert and K.-H. Höck, *Phys. Rev. B* **57**, 727 (1998).
- ²⁰J. P. Perdew and Y. Wang, *Phys. Rev. B* **45**, 13244 (1992).
- ²¹G. Kresse and J. Furthmüller, *Comput. Mater. Sci.* **6**, 15 (1996).
- ²²G. Kresse and D. Joubert, *Phys. Rev. B* **59**, 1758 (1999).
- ²³M. Losurdo, D. Barreca, G. Bruno, and E. Tondello, *Thin Solid Films* **384**, 58 (2001).

²⁴J. Heyd, G. E. Scuseria, and M. Ernzerhof, *J. Chem. Phys.* **118**, 8207 (2003); **124**, 219906 (2006); J. Paier, M. Marsman, K. Hummer, G. Kresse, I. C. Gerber, and J. G. Ángyán, *J. Chem. Phys.* **125**, 249901 (2006). The hybrid functional HSE06 is an exchange correlation functional combined as a fractional mixture of Fock and Perdew–Burke–Ernzerhof (PBE) exchange along with PBE correlation.

²⁵J. J. Quinn and R. A. Ferrell, *Phys. Rev.* **112**, 812 (1958).

²⁶P. Clauws and J. Vennik, *Phys. Stat. Solidi B* **66**, 553 (1974).

²⁷C. Sanchez, M. Henry, J. C. Grenet, and J. Livage, *J. Phys. C: Solid State Phys.* **15**, 7133 (1982).

Figure Captions

Fig. 1. Cyclic voltammograms showing current as a function of potential vs. Li^+ for an amorphous V_2O_5 film. Data were taken at the first and tenth measurement cycle. Arrows indicate voltage sweep direction.

Fig. 2. Chronopotentiometry data on potential vs. Li^+ as a function of intercalation parameter x for two as-deposited V_2O_5 films (solid curves) and for such films after ten voltammetric cycles (dashed curves).

Fig. 3. Calculated electronic density of states, per formula unit, of amorphous V_2O_5 as a function of energy. Zero energy was put at the top of the valence band. The curves denote total DOS as well as partial DOS from V and O atoms, as given in the figure.

Fig. 4. Electrochemical density-of-states (EDOS) as a function of potential for two amorphous V_2O_5 films (a) and computed total density-of-states (DOS) for the same material (b). The energy (E) scale is the same as in Fig 3 and is related to the potential (U) scale by $E = 6.15 - U$. Note that the vertical scales are different for the two panels.

Fig. 5. Electrochemical density of states (EDOS) for an as-deposited V_2O_5 film and a similar, pretreated film that has undergone ten voltammetric cycles.

Fig. 6. Energy-dependent optical absorption coefficient for amorphous V_2O_5 thin films with different amounts of intercalated Li^+ ions. Film thickness and intercalation parameter are denoted d and x , respectively.